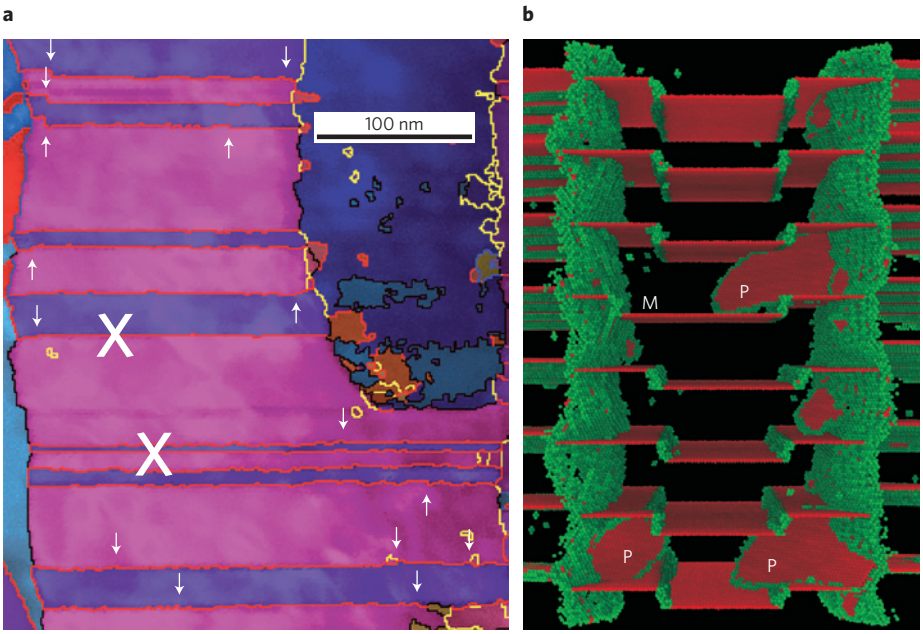

Figure 2 | Microstructure and deformation mechanisms of nanotwinned Cu. **a**, Inverse pole figure orientation mapping (IPFOM) high-resolution image of growth twins, twin boundaries and a GB. Arrows mark the location of selected kinks, and CTBs that are absent of defects are denoted with an 'X'. IPFOM is an electron-diffraction technique similar to dark-field transmission-electron-microscopy (TEM) imaging that Wang and colleagues adapted to work inside a field-emission TEM. The adapted technique is able to collect many thousands of diffraction patterns with their respective crystallographic orientations by rastering the images with a cone-shaped beam spot of ~1 nm. **b**, Simulation snapshot of the evolution of the microstructure in a columnar grain with kinked CTBs at ~1.7% tensile strain. The locations where kink migration and partial-dislocation emission from GBs occurred are denoted by M and P, respectively. Figure reproduced from ref. 10, © 2013 NPG.

have shown the emission of threading dislocations from GBs and their subsequent glide along slip directions parallel to the twin boundaries. Wang and co-authors now demonstrate that emitted threading dislocations readily transmit through perfect CTBs and annihilate in an opposite GB. It thus seems that CTBs have a dynamic character as the defects migrate along them, and that they facilitate the creation and proliferation of additional inhomogeneities within the crystal structure.

Clearly, the work of Wang and collaborators brings into question the appropriateness of existing atomistic and analytical models where twin boundaries have been treated as perfect interfaces. It further highlights the importance of a proper choice of assumptions when interpreting results from atomistic simulations in the context of experimental work and emphasizes that, with respect to mechanical properties, deformation and failure of materials, imperfections are almost all that matter. ❐

Julia R. Greer is at the Division of Engineering and Applied Sciences, California Institute of Technology, Pasadena, California 91125-8100, USA.
e-mail: jrgreer@caltech.edu

References

1. Nieh, T. G. & Wadsworth, J. *Scripta Metall. Mater.* **25,** 955–958 (1991).
2. Hall. E. O. *Proc. Phys. Soc. B* **64,** 742–753 (1951).
3. Petch, N. J. *J. Iron Steel Inst.* **174,** 25–28 (1953).
4. Hodge, A., Wang, Y-M. & Barbee, T. W. *J. Scripta Mater.* **59,** 163–166 (2008).
5. Lu, L. *et al. Acta Mater.* **57,** 5165–5173 (2009).
6. Jang, D., Li, X., Gao, H. & Greer, J. R. *Nature Nanotech.* **7,** 594–601 (2012).
7. Lu, K., Lu, L. & Suresh, S. *Science* **324,** 349–352 (2009).
8. Afanasyev, K. & Sansoz, F. *Nano Lett.* **7,** 2056–2062 (2007).
9. Li, X., Wei, Y., Lu, L., Lu, K. & Gao, H. *Nature* **464,** 877–880 (2010).
10. Morris Wang, Y. *et al. Nature Mater.* **12,** 697–702 (2013).
11. Mishin, Y., Mehl, M. J., Papaconstantopoulos, D. A., Voter, A. F. & Kress, J. D. *Phys. Rev. B* **63,** 224106 (2001).
12. Greer, J. R., Jang, D. & Gu, X. W. *JOM* **64,** 1241–1252 (2012).

VALLEYTRONICS

Electrons dance in diamond

In addition to manipulating the charge or spin of electrons, another way to control electric current is by using the 'valley' degree-of-freedom of electrons. The first demonstration of the generation, transport and detection of valley-polarized electrons in bulk diamond now opens up new opportunities for quantum control in electronic devices.

Christoph E. Nebel

Conventional electronics operate by exploiting the properties of the carriers of electric charge (electrons) in materials. Such properties result from the detailed interactions between electrons and the crystal lattice formed by atoms. The encoding of information using the charge of electrons, for example the absence or presence of electrons, is attractive as the electric charge can be easily manipulated and interrogated by electric fields. Next-generation devices will make use of quantum effects such as spins (spintronics and quantum computing), which work by controlling the spin angular momentum of electrons[1]. The advantage of using spins is that they are shielded from undesired electric fluctuations in the environment, making the information more robust and reproducible.

Atoms define the structure of a crystal lattice, and electrons interacting with each other and the atoms dictate the conduction properties of the solid. These properties form the basis of the band structure. In semiconductors the band structure contains the valence band where bonding electrons are located, these can be excited into the conduction band, which is separated from the valence band by

a forbidden energy gap (bandgap). The propagation of the bonding electrons is driven by a density gradient (diffusion) or an electric field (drift). The conduction band is the set of energy and momentum values a charge carrier can have as electrons travel through a crystal as waves, which are described by a momentum (which is a continuous variable) and a spin (which is a discrete index). It is possible for a crystal to have two or more axes that differ in their orientation, but are otherwise identical: such axes can support electron waves that are also identical apart from their direction (or, more precisely, their momentum). The conduction band contains 'valleys' in the energy spectrum. Different crystal axes support electrons with different momenta appearing as valleys in a plot of energy versus momentum. Valleys of this kind can trap electrons, however they are not trapped in a specific place, but into a preferred momentum — meaning that the valleys channel the flow of charge in a particular way. If there are two or more conduction- (or valence-) band valleys in momentum space, then confining charge carriers in one of these valleys allows the realization of valleytronic devices[1–4].

As in spintronics, there are two main challenges facing researchers trying to make valleytronic devices. The first is restricting electrons to one quantum number, which for valleytronics means localizing them to one momentum valley. This is also referred to as achieving valley polarization. The second challenge is to detect the resulting valley-polarized current. Creating valley polarization is rather less straightforward but has been shown for AlAs (ref. 5), bismuth[6], graphene[1–4] and recently for MoS_2 (refs 7–9). The degree of valley polarization is however limited and related valley-polarization time constants are too short for device applications (nanosecond regime for MoS_2).

Writing in *Nature Materials*, Isberg and co-workers report[10] for the first time the generation, transport (across macroscopic distances) and detection of valley-polarized electrons in bulk diamond with a relaxation time of 300 ns at 77 K. To achieve valley polarization in diamond, the authors used high electric fields and pulsed photogenerated electrons in a time-of-flight set-up where they also applied a magnetic field to detect the valley polarization dynamically. Key to their findings is the purity of diamond. Over recent years the quality of diamond has been optimized significantly[11] to a level that makes it superior for spintronic applications[12]. For example, ultrapure diamond is grown by a microwave-enhanced chemical vapour deposition technique, resulting in less than 10^{13} cm^{-3} extrinsic defects. It therefore shows excellent electronic properties.

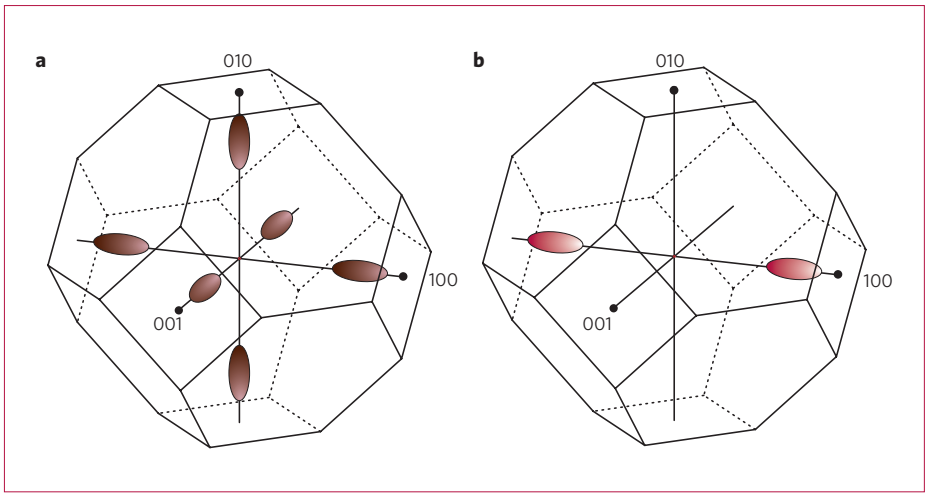

Figure 1 | Electronic band diagrams of diamond. **a**, Schematic picture of the first Brillouin zone of diamond, which shows that at low electric fields, all valleys (100, 010, 001) are equally occupied (as indicated by red ellipsoids). **b**, Applying high electric fields gives rise to (100)-valley polarization, which is parallel to the externally applied electric field. Figure reproduced from ref. 10, © 2012 NPG.

The conduction-band structure of diamond is similar to that of silicon (Fig. 1a), with six equivalent conduction-band valleys oriented along the {100} axes. Electrons in these valleys have a longitudinal effective mass of $m_l = 1.15m_0$ (where m_0 is the electron rest mass) and a transverse effective mass $m_t = 0.22m_0$ (ref. 13) generating a strong anisotropy of carrier propagation with respect to different crystal orientations. In diamond, intervalley phonon scattering requires interaction with longitudinal-acoustic or transverse-optical phonon modes (which are exceptionally high in energy, about 120 meV) close to the K point at the Brillouin zone boundary[14]. In comparison, the corresponding value is about 40 meV in Si. In diamond, the average time for scattering between valleys on the same axis is shorter than 1 ns due to a lower barrier of about 65 meV, and the average intravalley scattering by acoustic deformation potentials is shorter by about 1 ps due to the lack of a barrier.

Isberg and co-workers generate hot electrons by applying a high electric field parallel to one of the (100)-crystal orientations, which are subsequently scattered by intervalley phonons and thereby accumulate in the two valleys parallel to the electric field (Fig. 1b). The high electric field can be used to generate fully valley-polarized electrons in diamond with a lifetime of about 300 ns. The degree of polarization is dynamically detected by using the Hall angle that arises from the anisotropic mass tensor in the different valleys.

The first realization of valley-polarized electron states in diamond provides a promising route towards additional new quantum applications. The results of Isberg and colleagues demonstrate electrically controlled and dynamically measured valley polarization, and are promising for the realization of valleytronic-based devices in the future. ❐

Christoph E. Nebel is in Fraunhofer-Institute for Applied Solid State Physics (IAF), Tullastrasse 72, 79108 Freiburg, Germany.
e-mail: Christoph.Nebel@iaf.fraunhofer.de

References

1. Dyakonov, M. I. *Physica E* **35,** 246–250 (2006).
2. Rycerz, A., Tworzydlo, J. & Beenakker, C. W. J. *Nature Phys.* **3,** 172–175 (2007).
3. Xiao, D., Yao, W. & Niu, Q. *Phys. Rev. Lett.* **99,** 236809 (2007).
4. Akhmerov, A. R. & Beenakker, C. W. J. *Phys. Rev. Lett.* **98,** 157003 (2007).
5. Bishop, N. C. *et al. Phys. Rev. Lett.* **98,** 266404 (2007).
6. Zhu, Z. W., Collaudin, A., Fauque, B., Kang, W. & Behnia, K. *Nature Phys.* **8,** 89–94 (2012).
7. Zeng, H. L., Dai, J. F., Yao, W., Xiao, D. & Cui, X. D. *Nature Nanotech.* **7,** 490–493 (2012).
8. Mak, K. F., He, K. L., Shan, J. & Heinz, T. F. *Nature Nanotech.* **7,** 494–498 (2012).
9. Cao, T. *et al. Nature Commun.* **3,** 887 (2012).
10. Isberg, J. *et al. Nature Mater.* **12,** 760–764 (2013).
11. Balasubramanian, G. *et al. Nature Mater.* **8,** 383–387 (2009).
12. Jelezko, F. & Wrachtrup, J. *New J. Phys.* **14,** 105024–105026 (2012).
13. Löfas, H., Grigoriev, A., Isberg, J. & Ahuja, R. *AIP Advances* **1,** 032139 (2011).
14. Pavone, P. *et al. Phys. Rev. B* **48,** 3156–3163 (1993).